www.ietdl.org

Published in IET Electric Power Applications
Received on 18th October 2012
Revised on 3rd May 2013
Accepted on 21st May 2013
doi: 10.1049/iet-epa.2013.0091

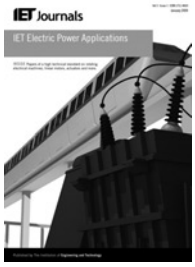

ISSN 1751-8660

Stator current model reference adaptive systems speed estimator for regenerating-mode low-speed operation of sensorless induction motor drives

Shady M. Gadoue[1,2], *Damian Giaouris*[3], *John W. Finch*[1]

[1]*School of Electrical and Electronic Engineering, Newcastle University, Newcastle upon Tyne, NE1 7RU, UK*
[2]*Department of Electrical Engineering, Faculty of Engineering, Alexandria University, Alexandria 21544, Egypt*
[3]*Chemical Process Engineering Research Institute (CPERI), Centre for Research and Technology Hellas (CERTH), Thermi-Thessaloniki 57001, Greece*
E-mail: shady.gadoue@ncl.ac.uk

Abstract: The performance of a stator current-based model reference adaptive systems (MRAS) speed estimator for sensorless induction motor drives is investigated in this study. The measured stator currents are used as a reference model for the MRAS observer to avoid the use of a pure integrator. A two-layer, online-trained neural network stator current observer is used as the adaptive model for the MRAS estimator which requires the rotor flux information. This can be obtained from the voltage or current models, but instability and dc drift can downgrade the overall observer performance. To overcome these problems of rotor flux estimation, an off-line trained multilayer feed-forward neural network is proposed here as a rotor flux observer. Hence, two networks are employed: the first is online trained for stator current estimation and the second is off-line trained for rotor flux estimation. Sensorless operation for the proposed MRAS scheme using current model and neural network rotor flux observers are investigated based on a set of experimental tests in the low-speed region. Using a neural network rotor flux observer to replace the current model is shown to solve the stability problem in the low-speed regenerating mode of operation.

1 Introduction

Sensorless vector controlled induction motor (IM) drives are being vigorously developed for high-performance industrial drive systems. Sensorless drives have been successfully applied in medium and high-speed regions, but low and zero speed operation is still a critical problem especially for IM drives [1, 2]. Numerous strategies have been described in the literature for rotor speed estimation in such drives [1, 3]. In general, these methods fall into two main categories: fundamental excitation and spectral analysis techniques [1, 4].

Fundamental model-based techniques for rotor speed estimation of IM drives make use of the instantaneous values of stator voltages and currents to estimate the flux linkage and the motor speed or position. These methods usually utilise a *d–q* model to describe the machine equations by assuming sinusoidal flux distribution and neglecting space harmonics [1]. These schemes usually work well above 2% of the base speed [1].

Model-based estimation strategies include open-loop estimators [3], observer-based schemes [5], sliding-mode observers [6–8], extended and unscented Kalman filters [9, 10], model reference adaptive systems (MRAS) [4, 11–14] and artificial intelligence (AI)-based methods [3, 15]. Recent work uses predictive current control for sensorless IM drives [16]. MRAS observers are well-established sensorless techniques that have attracted much attention because of their simplicity and direct physical interpretation. Various MRAS schemes have been proposed in the literature based on rotor flux [11], back electromotive force [12, 13], active or reactive power [13, 15] and stator current [14]. Improving the performance of these schemes at very low speed still remains challenging. The stability problem in the regenerating operation at low speed is another issue for sensorless IM drives. This problem has been extensively reported [4, 15, 17, 18].

AI techniques, especially neural networks (NNs), have been widely employed in various applications in the past two decades [19]. Various NN-based techniques have been successfully applied to sensorless drives [15, 20–26].

A sensorless full-order speed adaptive flux observer was originally proposed by Kubota *et al.* [5] based on adaptive control theory. This observer uses the stator-current error in speed estimation and does not suffer from drifting problems except if the gains are poorly selected. The adaptation mechanism is derived using Lyapunov's theorem and was shown to be based on a combination of the rotor flux vector and the stator-current vector error. Compared with a stator-current error-based MRAS estimator, the adaptive flux observer [5] needs more effort in the design stage to choose the adaptation loop parameters in addition to the gain matrix parameters [14].

However, as shown by Suwankawin and Sangwongwanich [27], stability problems at low speeds in the regenerating mode may appear when using the scheme proposed in [5] unless the gains are properly selected or unless the adaptation law is modified. A general stabilising gain for this observer was derived in [28]. The present paper introduces another approach based on NNs to solve the instability problems at low speed and during regeneration.

A stator-current MRAS scheme has been recently introduced by the authors for rotor speed identification of IM drives [29]. That was a modification of the stator resistance estimation system presented in [22]. In this scheme, the reference model comprises of the measured stator current components. This makes the reference model free of pure integration problems and insensitive to motor parameter variations. A two-layer linear NN stator current observer is used as an adaptive model where the rotor speed is one of the NN weights. A back-propagation learning algorithm is used to train the NN online to update the value of rotor speed so as to minimise the error between the measured and estimated currents [29].

Rotor flux is needed for stator current estimation in the adaptive model and conventionally either a voltage model (VM) [30] or a current model (CM) flux observer [22] has been employed. However, as described in [29, 31], the use of a CM gives instability in the regeneration. Furthermore, a VM is not suitable for low-speed applications. Therefore an off-line trained multilayer feed-forward NN is proposed in this paper to solve the flux estimation problem. By using this NN, flux estimation is independent of rotor speed and does not require the use of pure integration.

Early simulation results given in [29] clearly showed superior results when employing the NN flux observer in terms of stator resistance sensitivity and stability over the whole speed control range. The instability behaviour of the scheme in regeneration when using a CM flux observer was experimentally validated in [31] using only encoded results.

The purpose of this paper is to experimentally investigate the performance of the stator-current MRAS scheme based on two different flux estimation topologies, CM and NN, in sensorless mode of operation.

The proposed stator-current MRAS schemes using CM and NN flux observers are experimentally validated based on a set of benchmark experimental tests using a 7.5 kW vector controlled IM drive. In this paper, sensorless mode of operation is considered when the drive is running both at low speed and in the regenerating mode.

Experimental results show the great improvement in low-speed operation performance using the proposed MRAS speed estimator which employs NN flux observer especially for regeneration. Sensorless results also confirm the instability problem in speed estimation when employing the CM for flux estimation in the regenerating-mode low-speed region of operation.

2 NN stator-current MRAS observer

For the stator-current MRAS observer the reference model will consist of the measured stator currents [22, 29], and hence the IM itself works as a reference model. This has the advantages of avoiding pure integration and the estimator is less parameter sensitive. A stator current observer can be represented by a linear two-layer NN with the motor speed expressed as one of its weights. A back-propagation learning algorithm is used to minimise the error in current estimation and hence in generating the estimated speed.

The rotor flux of the induction machine can be expressed either based on stator or rotor equations.

The VM flux estimator is based on the stator equation, which estimates the rotor flux in the stationary reference frame from the monitored stator voltages and currents [3]

$$p\psi_{\mathrm{r}\alpha} = \frac{L_{\mathrm{r}}}{L_m}\{v_{\mathrm{s}\alpha} - R_{\mathrm{s}}i_{\mathrm{s}\alpha} - \sigma L_{\mathrm{s}}pi_{\mathrm{s}\alpha}\} \tag{1}$$

$$p\psi_{\mathrm{r}\beta} = \frac{L_{\mathrm{r}}}{L_m}\left\{v_{\mathrm{s}\beta} - R_{\mathrm{s}}i_{\mathrm{s}\beta} - \sigma L_{\mathrm{s}}pi_{\mathrm{s}\beta}\right\} \tag{2}$$

The CM is also used to obtain the rotor flux components in the stationary reference frame based on the rotor equations as [3]

$$p\hat{\psi}_{\mathrm{r}\alpha} = \frac{L_m}{T_{\mathrm{r}}}i_{\mathrm{s}\alpha} - \frac{1}{T_{\mathrm{r}}}\hat{\psi}_{\mathrm{r}\alpha} - \hat{\omega}_{\mathrm{r}}\hat{\psi}_{\mathrm{r}\beta} \tag{3}$$

$$p\hat{\psi}_{\mathrm{r}\beta} = \frac{L_m}{T_{\mathrm{r}}}i_{\mathrm{s}\beta} - \frac{1}{T_{\mathrm{r}}}\hat{\psi}_{\mathrm{r}\beta} + \hat{\omega}_{\mathrm{r}}\hat{\psi}_{\mathrm{r}\alpha} \tag{4}$$

The stator equations in the stationary reference frame can be written as

$$\sigma L_{\mathrm{s}}pi_{\mathrm{s}\alpha} = v_{\mathrm{s}\alpha} - R_{\mathrm{s}}i_{\mathrm{s}\alpha} - \frac{L_m}{L_{\mathrm{r}}}p\psi_{\mathrm{r}\alpha} \tag{5}$$

$$\sigma L_{\mathrm{s}}pi_{\mathrm{s}\beta} = v_{\mathrm{s}\beta} - R_{\mathrm{s}}i_{\mathrm{s}\beta} - \frac{L_m}{L_{\mathrm{r}}}p\psi_{\mathrm{r}\beta} \tag{6}$$

where σ is the leakage coefficient given by

$$\sigma = 1 - \frac{L_m^2}{L_{\mathrm{s}}L_{\mathrm{r}}} \tag{7}$$

Substituting the rotor (3) and (4) into (5) and (6) yields

$$\begin{aligned}\sigma L_{\mathrm{s}}pi_{\mathrm{s}\alpha} &= v_{\mathrm{s}\alpha} - R_{\mathrm{s}}i_{\mathrm{s}\alpha} \\ &\quad - \frac{L_m}{L_{\mathrm{r}}}\left\{-\frac{1}{T_{\mathrm{r}}}\hat{\psi}_{r\alpha} - \hat{\omega}_{\mathrm{r}}\hat{\psi}_{\mathrm{r}\beta} + \frac{L_m}{T_{\mathrm{r}}}i_{\mathrm{s}\alpha}\right\}\end{aligned} \tag{8}$$

$$\begin{aligned}\sigma L_{\mathrm{s}}pi_{\mathrm{s}\beta} &= v_{\mathrm{s}\beta} - R_{\mathrm{s}}i_{\mathrm{s}\beta} \\ &\quad - \frac{L_m}{L_{\mathrm{r}}}\left\{-\frac{1}{T_{\mathrm{r}}}\hat{\psi}_{\mathrm{r}\beta} + \hat{\omega}_{\mathrm{r}}\hat{\psi}_{\mathrm{r}\alpha} + \frac{L_m}{T_{\mathrm{r}}}i_{\mathrm{s}\beta}\right\}\end{aligned} \tag{9}$$

Hence, the stator current equations in the stationary reference frame can be written as

$$\sigma L_{\mathrm{s}}pi_{\mathrm{s}\alpha} = v_{\mathrm{s}\alpha} - R_{\mathrm{s}}i_{\mathrm{s}\alpha} + \frac{L_m}{L_{\mathrm{r}}T_{\mathrm{r}}}\hat{\psi}_{\mathrm{r}\alpha} + \frac{L_m}{L_{\mathrm{r}}}\hat{\omega}_{\mathrm{r}}\hat{\psi}_{\mathrm{r}\beta} - \frac{L_m^2}{L_{\mathrm{r}}T_{\mathrm{r}}}i_{\mathrm{s}\alpha} \tag{10}$$

$$\sigma L_{\mathrm{s}}pi_{\mathrm{s}\beta} = v_{\mathrm{s}\beta} - R_{\mathrm{s}}i_{\mathrm{s}\beta} + \frac{L_m}{L_rT_r}\hat{\psi}_{\mathrm{r}\beta} - \frac{L_m}{L_{\mathrm{r}}}\hat{\omega}_{\mathrm{r}}\hat{\psi}_{\mathrm{r}\alpha} - \frac{L_m^2}{L_{\mathrm{r}}T_{\mathrm{r}}}i_{\mathrm{s}\beta} \tag{11}$$

Equations (10) and (11) can be used to represent the stator current observer. The discrete form of these equations can

doi: 10.1049/iet-epa.2013.0091

be obtained by using the backward difference method as [2]

$$p\hat{i}_{s\alpha} = \frac{\hat{i}_{s\alpha}(k) - \hat{i}_{s\alpha}(k-1)}{T} \quad (12)$$

$$p\hat{i}_{s\beta} = \frac{\hat{i}_{s\beta}(k) - \hat{i}_{s\beta}(k-1)}{T} \quad (13)$$

where T is the sampling time. Substituting (12) and (13) into (10) and (11) yields

$$\begin{aligned}\hat{i}_{s\alpha}(k) = &\left\{1 - \frac{TR_s}{\sigma L_s} - \frac{TL_m^2}{\sigma L_s L_r T_r}\right\}\hat{i}_{s\alpha}(k-1) \\ &+ \frac{TL_m}{\sigma L_s L_r T_r}\hat{\psi}_{r\alpha}(k-1) \\ &+ \frac{TL_m}{\sigma L_s L_r}\hat{\omega}_r\hat{\psi}_{r\beta}(k-1) + \frac{T}{\sigma L_s}v_{s\alpha}(k-1)\end{aligned} \quad (14)$$

$$\begin{aligned}\hat{i}_{s\beta}(k) = &\left\{1 - \frac{TR_s}{\sigma L_s} - \frac{TL_m^2}{\sigma L_s L_r T_r}\right\}\hat{i}_{s\beta}(k-1) \\ &+ \frac{TL_m}{\sigma L_s L_r T_r}\hat{\psi}_{r\beta}(k-1) \\ &- \frac{TL_m}{\sigma L_s L_r}\hat{\omega}_r\hat{\psi}_{r\alpha}(k-1) + \frac{T}{\sigma L_s}v_{s\beta}(k-1)\end{aligned} \quad (15)$$

Hence, the stator current equations of the induction machine can be written as [22, 29, 30]

$$\begin{aligned}\hat{i}_{s\alpha}(k) &= w_1\hat{i}_{s\alpha}(k-1) + w_2\hat{\psi}_{r\alpha}(k-1) \\ &\quad + w_3\hat{\psi}_{r\beta}(k-1) + w_4 v_{s\alpha}(k-1) \\ \hat{i}_{s\beta}(k) &= w_1\hat{i}_{s\beta}(k-1) + w_2\hat{\psi}_{r\beta}(k-1) \\ &\quad - w_3\hat{\psi}_{r\alpha}(k-1) + w_4 v_{s\beta}(k-1)\end{aligned} \quad (16)$$

where

$$\begin{aligned}w_1 &= 1 - \frac{TR_s}{\sigma L_s} - \frac{TL_m^2}{\sigma L_s L_r T_r}; \quad w_2 = \frac{TL_m}{\sigma L_s L_r T_r}; \\ w_3 &= \frac{TL_m}{\sigma L_s L_r}\hat{\omega}_r; \quad w_4 = \frac{T}{\sigma L_s}\end{aligned} \quad (17)$$

where T is the sampling time for the stator current observer.

Equation (16) can be represented by a two-layer linear NN with weights as defined in (17) as shown in Fig. 1. This NN will represent the adaptive model for the stator-current MRAS scheme where w_3, which contains the rotor speed information, is adjusted online in such a way as to minimise the error between actual and estimated currents [29].

To derive the weight adjustment law of the NN stator current observer, define the energy function E to be minimised

$$E = \frac{1}{2}\varepsilon^2(k) \quad (18)$$

where

$$\begin{aligned}\varepsilon(k) &= i_s(k) - \hat{i}_s(k) = \left[\, i_{s\alpha}(k) - \hat{i}_{s\alpha}(k) \quad i_{s\beta}(k) - \hat{i}_{s\beta}(k) \,\right]^{T} \\ &= \left[\, \varepsilon_\alpha(k) \quad \varepsilon_\beta(k) \,\right]^{T}\end{aligned} \quad (19)$$

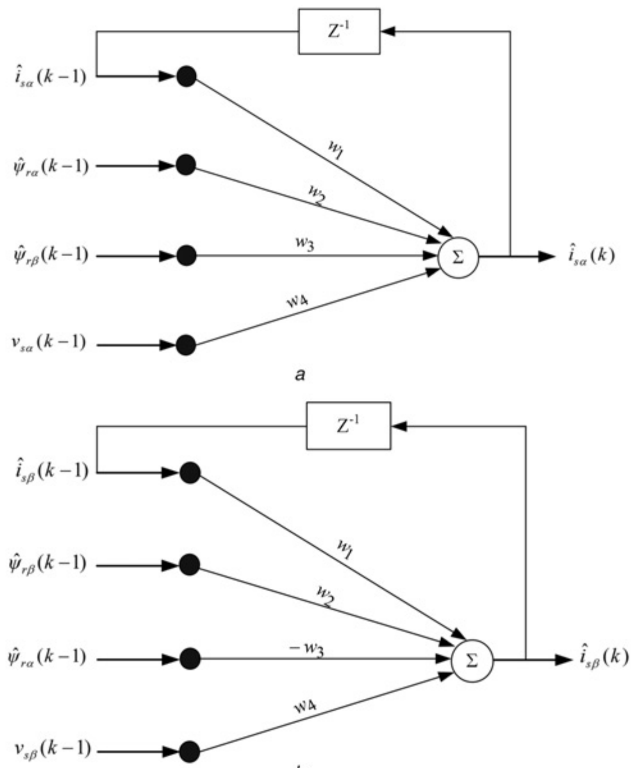

Fig. 1 *NN-based stator current observer discrete representation*

a α-axis
b β-axis

To obtain a minimum squared error between actual and estimated stator current, the weight adjustment has to be proportional to the negative of the error gradient with respect to the weight as

$$\Delta w_3 \propto -\frac{\partial E}{\partial w_3} \quad (20)$$

The weight adjustment law can be written as

$$\begin{aligned}\Delta w_3(k) &= -\eta\frac{\partial E}{\partial w_3} \\ &= \eta\Big\{\varepsilon_\alpha(k)\hat{\psi}_{r\beta}(k-1) - \varepsilon_\beta(k)\hat{\psi}_{r\alpha}(k-1)\Big\}\end{aligned} \quad (21)$$

where η is a positive constant called the learning rate. Large values of η may accelerate the NN learning and consequently fast convergence, but may cause oscillations in network output whereas low values will cause slow convergence. Therefore the value of η has to be chosen carefully to avoid instability.

The new weight can be written as

$$w_3(k) = w_3(k-1) + \Delta w_3(k) \quad (22)$$

To ensure accelerated convergence, the last weight change is added to the weight update as [3]

$$w_3(k) = w_3(k-1) + \Delta w_3(k) + \alpha\Delta w_3(k-1) \quad (23)$$

where α is a positive constant called the momentum constant.

The motor speed can be estimated from the weight w_3 as

$$\hat{\omega}_r(k) = \frac{\sigma L_s L_r}{T L_m} w_3(k) \tag{24}$$

It must be noted here that a similar approach was described in [30] using the VM for the rotor flux estimation. However, as will be described later, many problems are associated with using such model especially at low speed. In this paper, two other rotor flux estimators, based on CM and NN, will be employed and compared when the sensorless drive is operating at low speed and during regeneration.

3 Rotor flux estimation problem

Since rotor flux estimation is required for the stator-current MRAS scheme as shown in (16), a VM and CM flux observers can be used.

The VM was used in [30] for rotor flux estimation. However, the main drawback associated with VM implementation is the use of a pure integration which can cause dc drift, sensitivity to machine parameter variation, accurate stator voltage and current acquisition. These problems are not investigated in [30] and no low-speed results were shown especially during regeneration. Hence, the VM is unsuitable for low-speed operation.

The CM can also be used to avoid these problems. As given in (3) and (4) this model gives the rotor flux components in terms of stator current components and the rotor speed.

The block diagram of the NN-based stator-current MRAS scheme using a CM rotor flux observer is shown in Fig. 2.

Since rotor flux estimation using a CM depends on the estimated speed, any deterioration in speed estimation is fed back to the flux observer causing instability in the regenerating mode of operation. Deterioration of rotor flux estimation affects the stator current tracking causing instability of the speed estimation using the CM flux observer. Simulation results showing this unstable behaviour are obtained when the drive is subjected to a speed reversal command from 40 to -40 rpm at 25% load torque with nominal machine parameters. The speed estimation performance of the stator-current MRAS scheme using the CM rotor flux observer is shown in Fig. 3.

To overcome this problem another approach for rotor flux estimation is proposed here which uses an off-line trained NN. To estimate the rotor flux components in the stationary reference frame, a multilayer feed-forward NN [26] can be used.

This network is an 8-25-2 multilayer feed-forward NN as shown in Fig. 4. The number of neurons in the hidden layer is chosen by a trial and error technique. The inputs to the network are the present and past values of the α–β components of the stator voltage and current in the stationary reference frame. The output layer of the NN consists of two neurons representing the rotor flux components in the stationary reference frame. Since the case is approximating a non-linear function with bipolar input/output pattern, hyperbolic tangent (Tan-Sigmoid) activation functions is used in both hidden and output layers. Training data were obtained based on experimental data by running the encoded vector drive in the low-speed region (100 to -100 rpm) including zero speed at different load levels ranging from 0 to 25% of the rated load [26]. Hence, an NN, which is suitable for general purpose IM drives applications, is developed which focuses on the behaviour at relatively light load. This suits low speed, low torque applications such as fans, centrifugal pumps and blowers. Small and large references speed changes were applied to the drive during the training phase to include all the possible operating conditions.

The reference vector control stator voltages and measured stator currents are transformed from three phase (a, b, c) to two phase (α, β) for the NN training data. A low pass filter

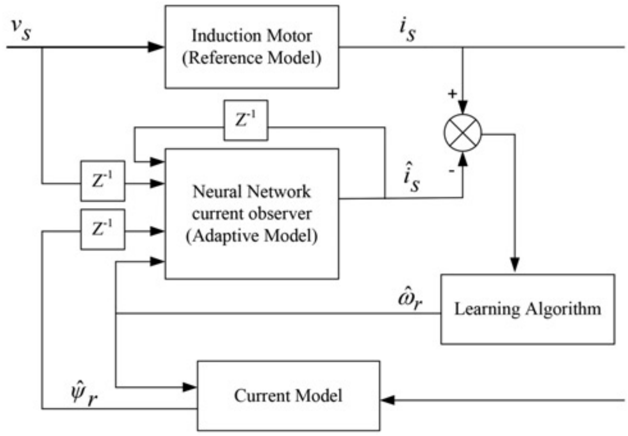

Fig. 2 *NN-based stator-current MRAS speed observer using CM flux observer*

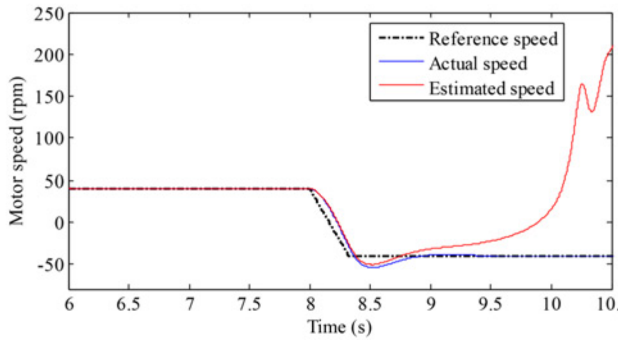

Fig. 3 *NN stator-current MRAS speed estimation performance in the regenerating mode using CM flux observer; simulation*

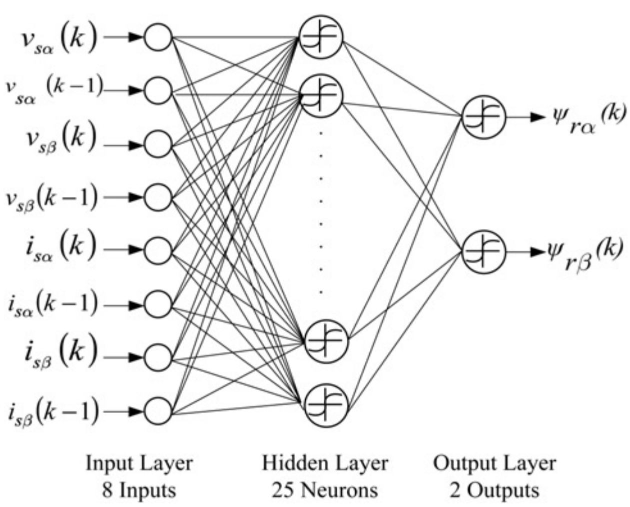

Fig. 4 *NN rotor flux observer*

IET Electr. Power Appl., 2013, Vol. 7, Iss. 7, pp. 597–606
doi: 10.1049/iet-epa.2013.0091

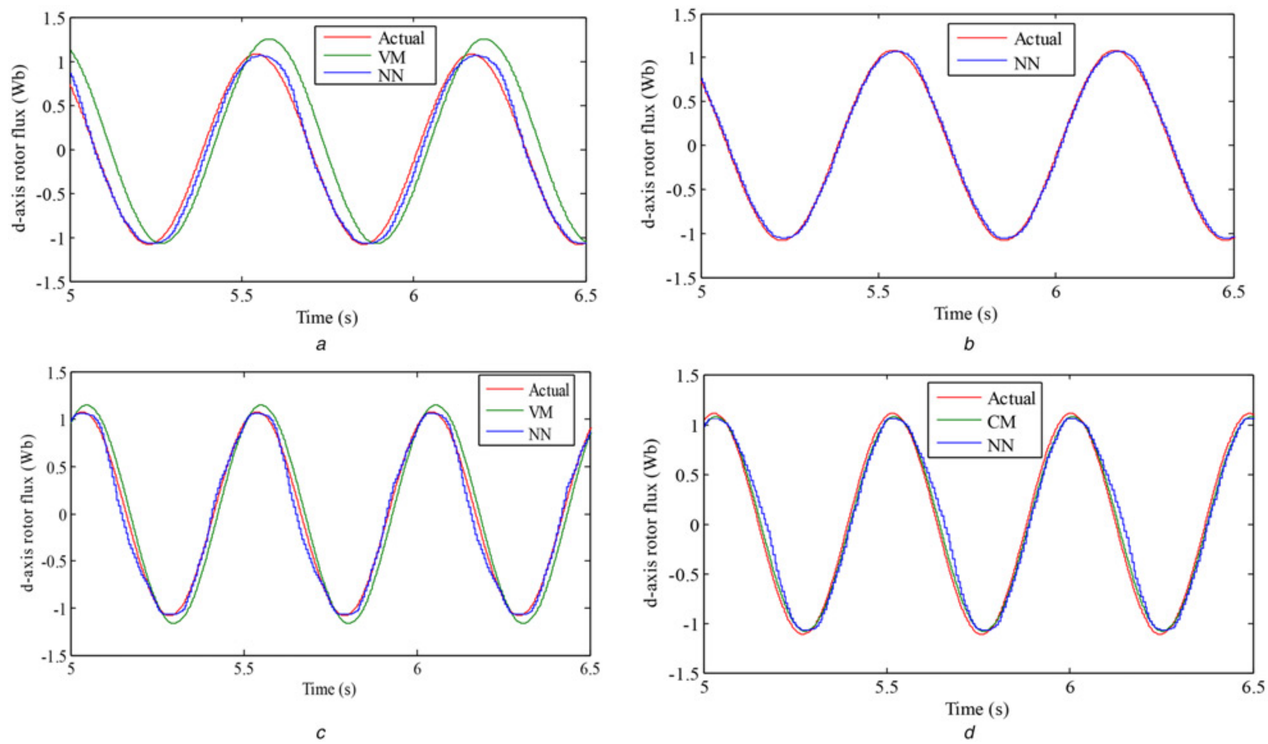

Fig. 5 *NN observer simulation testing*

No-load
a R_s 50% variation
b R_r 50% variation
25% load
c R_s 25% variation
d R_r 25% variation

(LPF) with 40 rad/s cut-off frequency was used to remove drift and noise from the reference stator voltage signals. The present and past samples of filtered stator voltages and stator currents components are obtained, which will be used as inputs to the NN model.

The outputs from the CM, which are obtained from stator currents components and encoder speed, are used as target values for the NN. This is an effective way to obtain the correct values of the rotor flux, since the obtained signals are relatively noise and harmonic-free including all the drive non-linearities. Moreover, the CM flux observer produces accurate flux estimation at low speed.

Since the measurements are generated at different scales for voltage, current and flux, scaling of the data variables is necessary to increase the numerical stability of the data processing. Furthermore, the scaling level is determined by the type of activation function being used. With hyperbolic tangent sigmoid function used in the hidden layer of the NN, training data have to be normalised to lie in the range between -1 and 1. The training is performed off-line with Matlab-Simulink using the Levenberg–Marquardt training algorithm. A 5000 input/output pattern was used to train the NN. After the training the mean squared error (MSE) between targets and NN outputs decays to a satisfactory level (4.5×10^{-4}) after about 2200 epochs.

The NN observer is best trained on the actual motor and inverter used, but in mass production this may not be practical. If the drive is designed as a single unit, then the NN observer would only have to cope with any parameter variations, which occur during the production run. Some further tolerance could be built-in by training on a range of motors.

This is a disadvantage of the proposed method, which would become more marked where an integrated drive is not feasible. Maybe a single inverter controller is to be used with a range of motor ratings. If a single training session were used then the performance of the NN observer would be poorer at extremes of the range of sizes. One compromise would be to train the observer on a number of motors. Then, during commissioning select using the motor's nameplate rating the particular set of NN parameters deployed.

The proposed NN flux observer is trained to match the performance of the CM, which is free from stator resistance

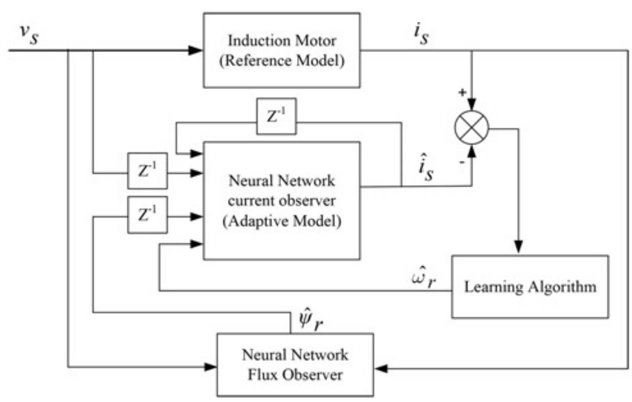

Fig. 6 *NN-based stator-current MRAS speed observer with NN flux observer*

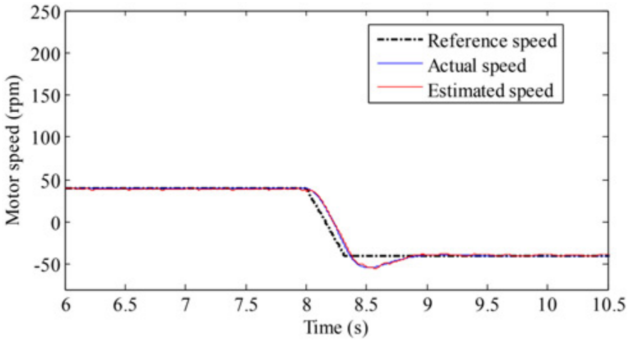

Fig. 7 *NN stator-current MRAS speed estimation performance in the regenerating mode using NN flux observer; simulation*

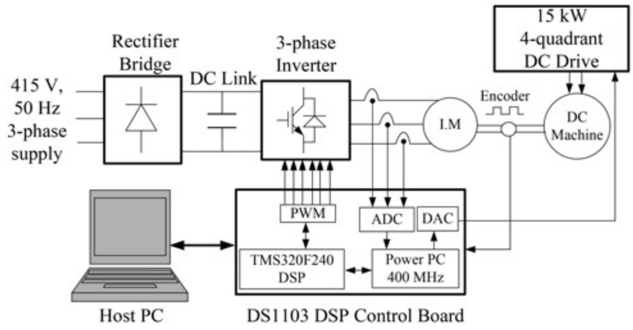

Fig. 8 *Experimental system platform*

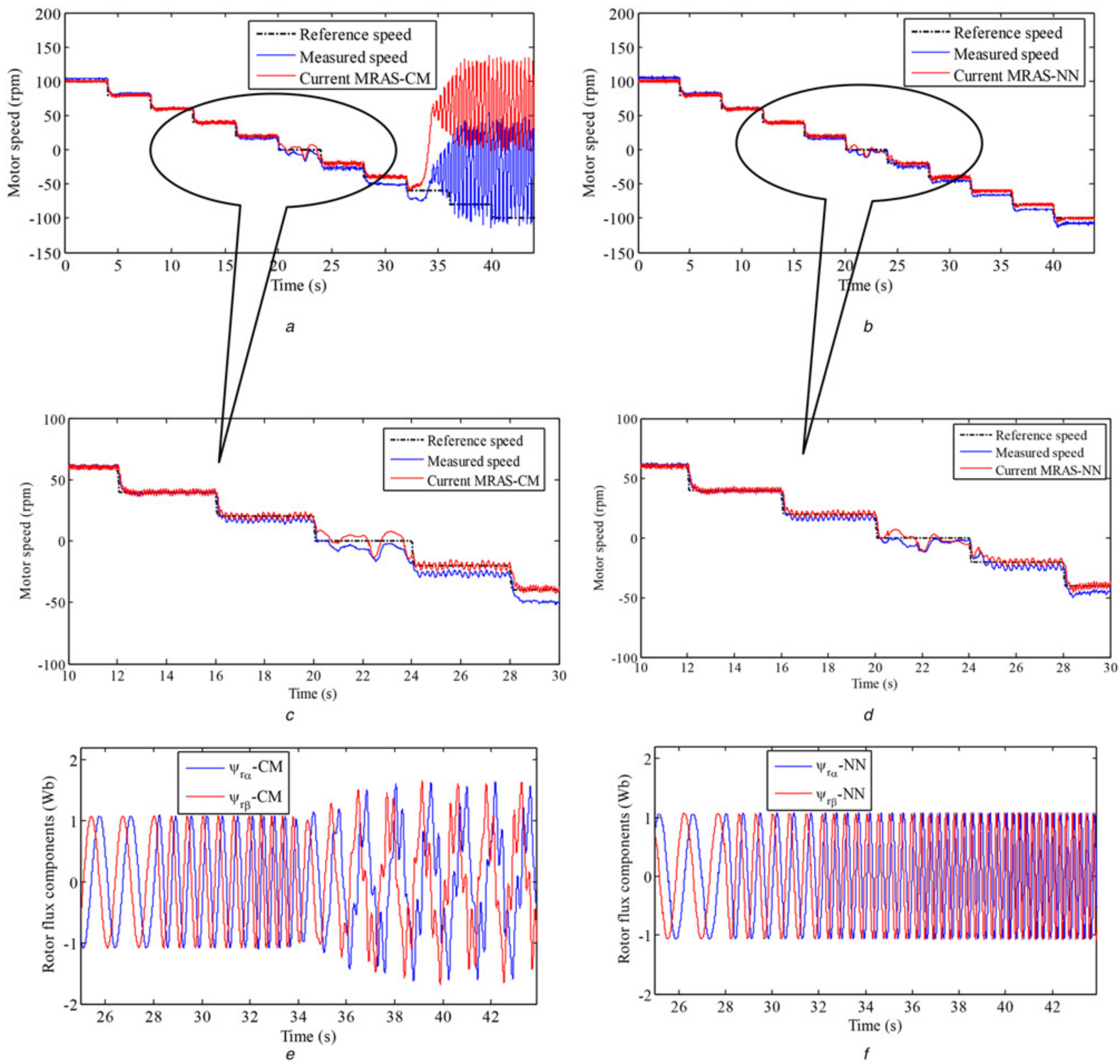

Fig. 9 *Sensorless performance for test 1, 12.5% load*

Speed response
a and *c* Stator-current MRAS-CM
b and *d* Stator-current MRAS-NN
Rotor flux estimation at regeneration
e CM
f NN

doi: 10.1049/iet-epa.2013.0091

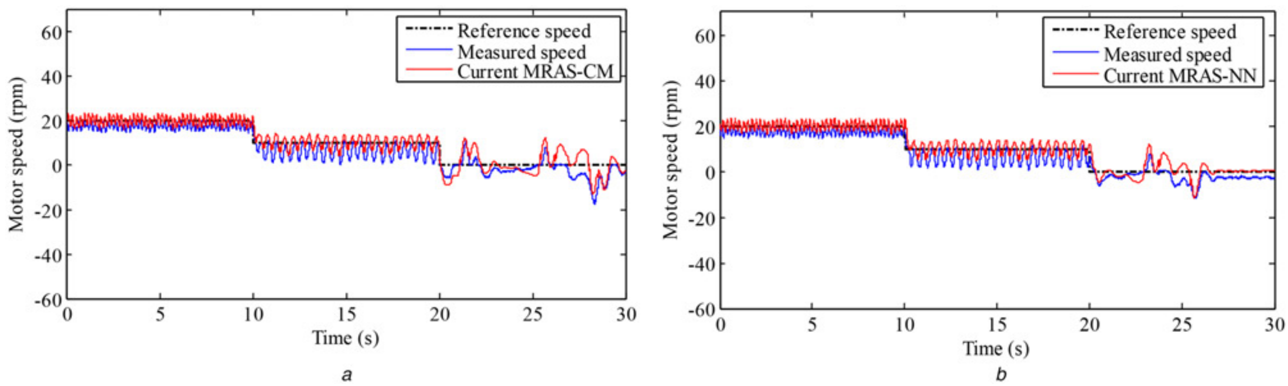

Fig. 10 *Sensorless performance for test 2, 10% load*

a Stator-current MRAS-CM
b Stator-current MRAS-NN

dependency and dc drift problems. Once the NN is trained it accurately matches the CM.

To test the NN observer sensitivity to parameter variation, simulations have been conducted with variations in R_s and R_r. These two parameters are the most crucial parameters that affect speed estimation especially at low speed. The performance of both observers is compared with the actual rotor flux output from the motor model when the vector control drive is working in encodered mode with and without load. The performance of VM and NN flux observers for 50% increase in R_s at no-load and for a 25% increase in R_s at 25% load is shown in Figs. 5*a* and *c*, respectively, where the NN shows less sensitivity to R_s variation than the VM. NN observer also shows good performance with 50% R_r variation at no-load as shown in Fig. 5*b*. With a 25% variation in R_r at 25% load, the CM is

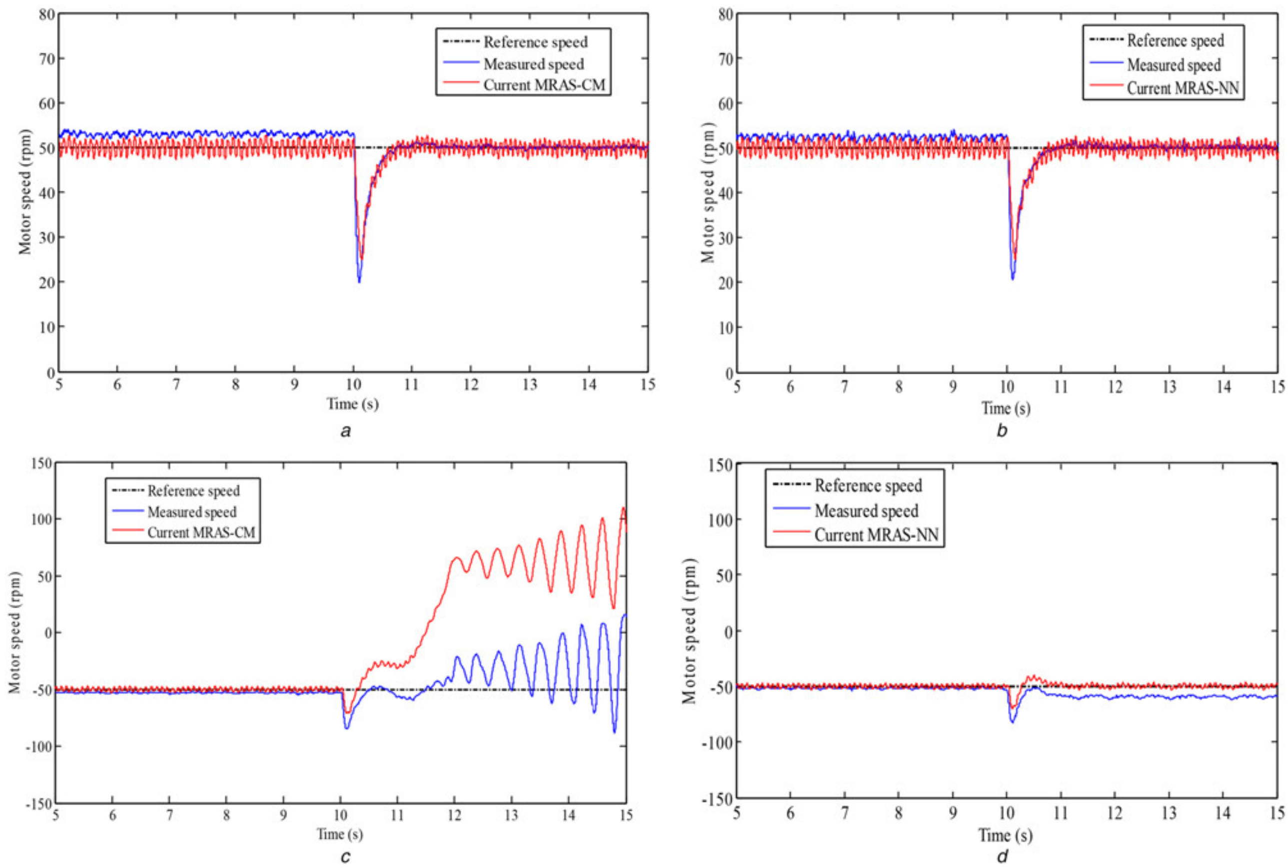

Fig. 11 *Sensorless performance for test 3, 20% load*

50 rpm
a Stator-current MRAS-CM
b Stator-current MRAS-NN
−50 rpm
c Stator-current MRAS-CM
d Stator-current MRAS-NN

slightly affected by this change, and since the NN was trained to match the CM performance it is similarly affected as shown in Fig. 5*d*. These results, shown in Fig. 5, demonstrate that the NN observer can handle the parameter variation problem with a good level of robustness.

However, unlike the CM, the NN is able to estimate the values of the rotor flux components without needing rotor speed information. Hence, it is possible to use the proposed NN for rotor flux estimation in the new MRAS scheme.

The block diagram of the stator-current MRAS scheme employing an NN for rotor flux estimation is shown in Fig. 6. In this scheme, two NN are used, an online-trained linear NN for stator current estimation and an off-line trained non-linear NN for rotor flux estimation. Compared with the unstable performance shown in Fig. 3, a stable performance for regeneration has been obtained using this scheme as shown Fig. 7.

4 Experimental results

In this section, the new stator-current MRAS scheme based on CM and NN flux observers is experimentally demonstrated in the sensorless mode of operation. The experimental system platform is shown in Fig. 8. It consists of a 7.5 kW, 415 V, delta-connected three-phase IM loaded by a 9 kW, 240 V, 37.5 A separately excited dc load machine controlled by a 15 kW four-quadrant dc drive. The induction machine parameters are given the Appendix.

A dSPACE DS1103 control board is used to control the IM, Hall effect current sensors are used to measure the motor line currents. The actual motor speed is measured by a 5000 pulses/revolution incremental optical encoder. The inverter switching frequency is 15 kHz, with a dead time period of 1.5 μs, and the vector control is executed with the same sampling frequency. The observer and the speed control loop have a sampling frequency of 5 kHz and the speed measurement is executed with a sampling frequency of 250 Hz.

The main focus of this paper is given to the sensorless operation of the proposed scheme at low speed and with regeneration. The two structures of the new scheme will be compared: current MRAS-CM using CM flux observer (Fig. 2) and current MRAS-NN using NN rotor flux observer (Fig. 6). In the following tests, the estimated speed is used for speed control and field orientation where the drive is working as sensorless indirect rotor flux oriented. The encoder speed is used for comparison purposes only.

Tests are conducted at low speed and at or around the zero speed region based on recommended benchmark tests [26, 32, 33]. Selected experimental results for the tests are shown in the following sections.

4.1 Test 1 – stair case speed transients from 100 to 0 rpm to −100 rpm at 12.5% load

In this test, the sensorless vector control drive is subjected to a stair case speed demand from 100 rpm to zero speed in a series of five 20 rpm steps continuing to −100 rpm, at 12.5% load.

The performance of CM- and NN-based schemes is shown in Figs. 9*a–d*. The stator-current MRAS-CM scheme shows instability in the regenerating operation whereas the stator-current MRAS-NN scheme shows stable operation. Using an NN for rotor flux estimation gives stable speed

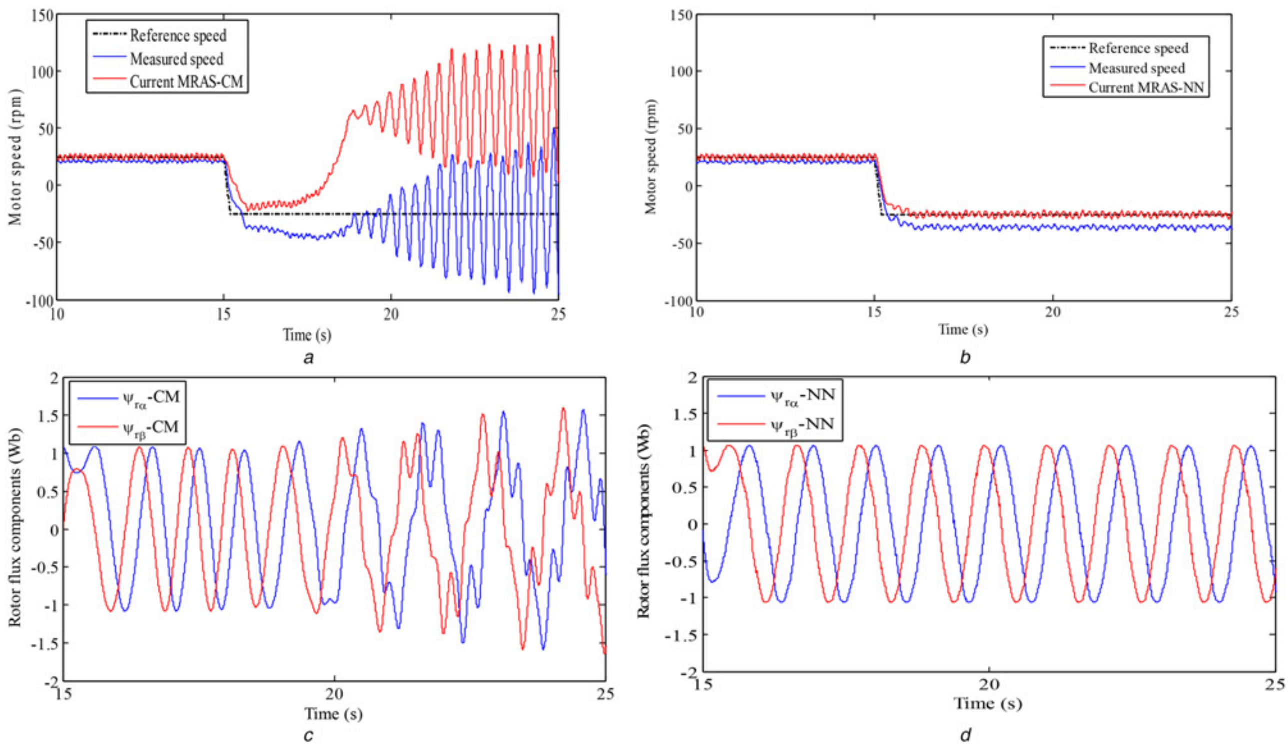

Fig. 12 *Sensorless performance for test 4, ±25 rpm reversal, 25% load*
a Stator-current MRAS-CM
b Stator-current MRAS-NN
Rotor flux estimation performance at regeneration
c CM
d NN

doi: 10.1049/iet-epa.2013.0091

estimation performance in the regenerating mode since flux estimation is independent of the estimated speed. This improves stator current tracking leading to stable speed estimation performance. Rotor flux estimation performances for CM and NN in regeneration are shown in Figs. 9*e* and *f*.

4.2 Test 2 – speed step down from 20 to 0 rpm in three steps each of 10 rpm

The results of this test at 10% load are shown in Figs. 10*a* and *b*. Better zero speed performance is obtained from the stator-current MRAS-NN scheme compared with the CM-based scheme. This is due to better rotor flux estimation using the NN at zero speed.

4.3 Test 3 – sensorless load disturbance rejection

Sensorless performance of the stator current-based schemes for 20% load torque disturbance rejection at 50 rpm is shown in Figs. 11*a* and *b*. Similar response is obtained from the two schemes. To examine the sensorless performance at regeneration, both stator current-based MRAS schemes are subjected to a 20% load torque application at -50 rpm. Results shown in Figs. 11*c* and *d* reveal that the instability obtained from the stator-current MRAS-CM with regeneration is completely removed by using the NN rotor flux observer.

4.4 Test 4 – speed reversal with load

This last test shows the drive performance for a very low speed reversal under load torque. A ± 25 rpm speed reversal demand was applied to the drive when working at 25% load. Unstable performance is obtained from the CM-based scheme in contrast to the stable performance for the NN-based scheme as shown in Figs. 12*a* and *b*. CM and NN flux estimation performance is shown in Figs. 12*c* and *d*.

5 Conclusions

This paper has experimentally investigated the sensorless performance of a stator current-based MRAS estimator with different rotor flux observers. Using a VM causes problems at low speed because of stator resistance sensitivity and the need for pure integration for flux. A CM can be used instead to estimate the rotor flux from the measured stator currents and the estimated speed. However, any deterioration in speed estimation is fed back to the CM flux observer causing instability in the regenerating mode of operation. Hence, a multilayer feed-forward NN is used to overcome this problem for rotor flux estimation from present and past samples of the stator voltage and current. Using the NN flux observer gives less sensitivity to stator resistance variations compared with the VM. Since the flux estimation is independent of the rotor speed stable operation has been obtained for regeneration.

The proposed schemes have been experimentally validated using a 7.5 kW vector controlled IM drive. These results confirm the improvement in sensorless performance using the new scheme at low speed with stable regeneration performance.

6 References

1 Finch, J.W., Giaouris, D.: 'Controlled AC electrical drives', *IEEE Trans. Ind. Electron.*, 2008, **55**, (2), pp. 481–491

2 Holtz, J., Quan, J.: 'Drift and parameter compensated flux estimator for persistent zero stator frequency operation of sensorless controlled induction motors', *IEEE Trans. Ind. Appl.*, 2003, **39**, (4), pp. 1052–1060

3 Vas, P.: 'Sensorless vector and direct torque control' (Oxford University Press, New York, 1998)

4 Ravi Teja, A.V., Chakraborty, C., Maiti, S., Hori, Y.: 'A new model reference adaptive controller for four quadrant vector controlled induction motor drives', *IEEE Trans. Ind. Electron.*, 2012, **59**, (10), pp. 3757–3767

5 Kubota, H., Matsuse, K., Nakano, T.: 'DSP-based speed adaptive flux observer of induction motor', *IEEE Trans. Ind. Appl.*, 1993, **29**, (2), pp. 344–348

6 Ghanes, M., Zheng, G.: 'On sensorless induction motor drives: slidingmode observer and output feedback controller', *IEEE Trans. Ind. Electron.*, 2009, **56**, (9), pp. 3404–3413

7 Comanescu, M., Xu, L.: 'Sliding mode MRAS speed estimators for sensorless vector control of induction machine', *IEEE Trans. Ind. Electron.*, 2006, **53**, (1), pp. 146–153

8 Vieira, R., Gastaldini, C., Azzolin, R., Gründling, H.: 'Discrete-time sliding mode speed observer for sensorless control of induction motor drives', *IET Electr. Power Appl.*, 2012, **6**, (9), pp. 681–688

9 Barut, M., Demir, R., Zerdali, E., Inan, R.: 'Real-time implementation of bi input-extended Kalman filter-based estimator for speed-sensorless control of induction motors', *IEEE Trans. Ind. Electron.*, 2012, **59**, (11), pp. 4197–4206

10 Jafarzadeh, S., Lascu, C., Fadali, M.: 'State estimation of induction motor drives using the unscented Kalman filter', *IEEE Trans. Ind. Electron.*, 2012, **59**, (11), pp. 4207–4216

11 Schauder, C.: 'Adaptive speed identification for vector control of induction motors without rotational transducers', *IEEE Trans. Ind. Appl.*, 1992, **28**, (5), pp. 1054–1061

12 Rashed, M., Stronach, A.F.: 'A stable back-EMF MRAS-based sensorless low speed induction motor drive insensitive to stator resistance variation', *IEE Proc. Electr. Power Appl.*, 2004, **151**, (6), pp. 685–693

13 Peng, F., Fukao, T.: 'Robust speed identification for speed-sensorless vector control of induction motors', *IEEE Trans. Ind. Appl.*, 1994, **30**, (5), pp. 1234–1240

14 Orlowska-Kowalska, T., Dybkowski, M.: 'Stator-current-based MRAS estimator for a wide range speed-sensorless induction-motor drive', *IEEE Trans. Ind. Electron.*, 2010, **57**, (4), pp. 1296–1308

15 Maiti, S., Verma, V., Chakraborty, C., Hori, Y.: 'An adaptive speed sensorless induction motor drive with artificial neural network for stability enhancement', *IEEE Trans. Ind. Inf.*, 2012, **8**, (4), pp. 757–766

16 Guzinski, J., Abu-Rub, H.: 'Speed sensorless induction motor drive with predictive current controller', *IEEE Trans. Ind. Electron.*, 2013, **60**, (2), pp. 699–709

17 Zaky, M.S.: 'Stability analysis of speed and stator resistance estimators for sensorless induction motor drives', *IEEE Trans. Ind. Electron.*, 2012, **59**, (2), pp. 858–870

18 Etien, E., Chaigne, C., Bensiali, N.: 'On the stability of full adaptive observer for induction motor in regenerating mode', *IEEE Trans. Ind. Electron.*, 2010, **57**, (5), pp. 1599–1608

19 Bose, B.K.: 'Neural network applications in power electronics and motor drives – an introduction and perspective', *IEEE Trans. Ind. Electron.*, 2007, **54**, (1), pp. 14–33

20 Ben-Brahim, L., Tadakuma, S., Akdag, A.: 'Speed control of induction motor without rotational transducers', *IEEE Trans. Ind. Appl.*, 1999, **35**, (4), pp. 844–850

21 Campbell, J., Sumner, M.: 'Practical sensorless induction motor drive employing an artificial neural network for online parameter adaptation', *IEE Proc. Electr. Power Appl.*, 2002, **149**, (4), pp. 255–260

22 Karanayil, B., Rahman, M.F., Grantham, C.: 'Online stator and rotor resistance estimation scheme using artificial neural networks for vector controlled speed sensorless induction motor drives', *IEEE Trans. Ind. Electron.*, 2007, **54**, (1), pp. 167–176

23 Cirrincione, M., Pucci, M.: 'An MRAS-based sensorless high-performance induction motor drive with a predictive adaptive model', *IEEE Trans. Ind. Electron.*, 2005, **52**, (2), pp. 532–551

24 Cirrincione, M., Pucci, M., Cirrincione, G., Capolino, G.A.: 'Sensorless control of induction machines by a new neural algorithm: the TLS EXIN neuron', *IEEE Trans. Ind. Electron.*, 2007, **54**, (1), pp. 127–149

25 Cirrincione, M., Pucci, M., Cirrincione, G., Capolino, G.: 'A new adaptive integration methodology for estimating flux in induction machine drives', *IEEE Trans. Power Electron.*, 2004, **19**, (1), pp. 25–34

26 Gadoue, S.M., Giaouris, D., Finch, J.W.: 'Sensorless control of induction motor drives at very low and zero speed using neural network flux observers', *IEEE Trans. Ind. Electron.*, 2009, **56**, (8), pp. 3029–3039
27 Suwankawin, S., Sangwongwanich, S.: 'A speed-sensorless IM drive with decoupling control and stability analysis of speed estimation', *IEEE Trans. Ind. Electron.*, 2002, **49**, (2), pp. 444–455
28 Sangwongwanich, S., Suwankawin, S., Koonlaboon, S.: 'A unified speed estimation design framework for sensorless AC motor drives based on positive-real property'. Power Conversion Conf. – Nagoya, 2007 (PCC '07), 2–5 April 2007, pp. 1111–1118
29 Gadoue, S.M., Giaouris, D., Finch, J.W.: 'A neural network based stator current MRAS observer for speed sensorless induction motor drives'. Proc. IEEE Int. Symp. Industrial Electronics, Cambridge, UK, 2008, pp. 650–655
30 Sobczuk, D., Grabowski, P.: 'DSP implementation of neural network speed estimator for inverter fed induction motor'. Proc. 24th Annual Conf. IEEE Industrial Electronics Society, 1998 (IECON '98), 31 August–4 September 1998, vol. 2, pp. 981–985
31 Gadoue, S.M., Giaouris, D., Finch, J.W.: 'An experimental assessment of a stator current MRAS based on neural networks for sensorless control of induction machines'. Proc. 2011 Symp. Sensorless Control for Electrical Drives, Birmingham, UK, 2011, pp. 102–106
32 Ohyama, K., Asher, G.M., Sumner, M.: 'Comparative experimental assessment for high-performance sensorless induction motor drives'. Proc. IEEE Int. Symp. Industrial Electronics (ISIE '99), 1999
33 Ohyama, K., Asher, G.M., Sumner, M.: 'Comparative analysis of experimental performance and stability of sensorless induction motor drives', *IEEE Trans. Ind. Electron.*, 2006, **53**, (1), pp. 178–186

7 Appendix

7.1 Motor parameters

A 7.5 kW, three-phase, 415 V, delta-connected, 50 Hz, four-pole, star equivalent parameters are: $R_s = 0.7767\ \Omega$, $R_r = 0.703\ \Omega$, $L_s = 0.10773$ H, $L_r = 0.10773$ H, $L_m = 0.10322$ H and $J = 0.22$ kgm^2.

doi: 10.1049/iet-epa.2013.0091